BioCore Exploring Scientific Community

International Journal of Biotechnology and Bioengineering

Research Article ISSN 2475-3432

Simple and rapid Simultaneously Colorimetric determination of betamethasone and nephazoline based on partial least square using gold nanoparticle probe

Morteza Bahram[1], Sakineh Alizadeh*[2]

[1]*Department of chemistry, Faculty of Science, Urmia University, 5715175976, Urmia, Iran*
[2]*Department of Analytical chemistry, Faculty of Chemistry, Bu-Ali Sina University, 65178638695, Hamadan, Iran*

Abstract

Gold nanoparticles (Au NPs) have attracted enormous scientific and technological interest due to their ease of synthesis, chemical stability, and unique optical properties. In this work the absorbance of the Au NPs at 520 nm decreased and in 640 increased with the increase in the concentration of betamethasone (BET) and nephazoline (NEP). The rate of absorbance change in these drugs is difference. For this reason we can simultaneously determine the BET and NEP. The color change of the Au NPs with different concentrations of these drugs could make it convenient to be observed by the naked eye. The formation of Au NPs in the presence of citrate was monitored by transmission electron microscopy (TEM) and UV-Vis spectroscopy. The experimental conditions were optimized to obtain the highest yield for nanoparticle formation. Partial least square (PLS) regression as an efficient multivariate spectral calibration method was employed to make a connection between the SPR spectra of the generated Au NPs. The number of PLS latent variables was optimized by leave-one-out cross-validation utilizing prediction residual error sum of square (PRESS). This method allowed the determination of BET and NEP in the range of 0.05-13 µg / mL (R_2 = 0.9907) and 13-133.3 µg / mL (R_2 = 0.9906), with a low detection limit of 0.006 and 0.14 µg / mL (S/N = 5), respectively. This method was found to be sensitive and selective and was applied for the determination of BET and NEP in serum and Eye drops.

Keywords: Naphazoline, Betamethasone, Gold Nanoparticles, Pls, Sensor, Simultaneously Colorimetric Determination

***Corresponding author: Sakineh Alizadeh**
Department of Analytical chemistry, Faculty of Chemistry, Bu-Ali Sina University, 65178638695, Hamadan, Iran
Tel/ fax: +98 441 2972143
E-mail: solmaz.alizade@gmail.com

Citation: Sakineh Alizadeh et al.(2018), Simple and rapid Simultaneously Colorimetric determination of betamethasone and nephazoline based on partial least square using gold nanoparticle probe. Int J Biotech & Bioeng 4:2, 23-35.

Received: January 8, 2018, **Accepted:** January 18, 2018, **Published:** February 10, 2018

Introduction

Au nanoparticles (Au NPs) with high stability among the other metal nanoparticles have great interest due to their using in many fields such as sensors, biosensors, medicine, catalysis and many emerging areas of nanotechnology [1–3]. AuNPs are also useful colorimetric probes because of their distance-dependent optical properties and extremely high extinction coefficients at visible region [4, 5] which closely rely on their unique surface Plasmon resonance from red to blue, corresponding to their dispersion and aggregation states [5], respectively. Based on this principle, several colorimetric methods have been developed for the detection of ions [6], biomolecules [7], 2, 4, 6-trinitrotoluene (TNT) [8], drugs [9] and melamine [10].

In order to perform a global analysis on the spectral overlapping of total a flat oxins and simultaneous determination of them, chemometric methods must be employed. Recently, chemometric methods such as principal component regression) PCR), partial least square (PLS) and artificial neural network (ANN) have found increasing applications for multicomponent determinations [11–13].

Partial least squares (PLS) regression can allow simultaneous spectrophotometric determination of several drugs as well as improve the data handling process of complex chemical systems [14].

PLS calibration of a multicomponent system can be performed in two different ways, PLS1 and PLS2. The use of PLS2 has a few advantages. Firstly, there is one common set of PLS factors for all analytes. This simplifies the procedure and interpretation and allows for simultaneous graphical inspection. Secondly, when the analyte concentrations are strongly correlated, one may expect that the PLS2 model is more robust than separate PLS1 models. Finally, when the number of analytes is large the development of a single PLS2 model is performed much quicker than that of many separate PLS1 models [14].

Betamethasone (BET) is a potent glucocorticoid steroid with anti-inflammatory and immunosuppressive properties. Unlike other drugs with these effects, BET does not cause water retention [15]. It is applied as a topical cream, ointment, foam, lotion or gel to treat itching. BET sodium phosphate is sometimes prescribed as an intramuscular injection (I.M) for itching from various ailments, including allergic reactions to poisonivy and similar plan [16]. BET eye drops and ointment are used to treat short-term inflammatory eye conditions. They are usually prescribed by an eye specialist. They contain a corticosteroid (sometimes called a 'steroid') which helps relieve inflammation, redness and irritation [17].

The United States Pharmacopoeia (USP) 29 prescribes reverse phase high performance liquid chromatography (RP-HPLC) method for determination of BET dipropionate in cream, lotion and ointment [18]. Different liquid chromatographic methods have been reported for determination of BET valerate alone or in combination in different formulations [18, 19]. Nephazoline (NEP) is a sympathomimetic agent with marked alpha adrenergic activity. It is a vasoconstrictor with a rapid action in reducing swelling when applied to mucous membrane. It acts on alpha-receptors in the arterioles of the conjunctive to produce constriction, resulting in decreased congestion. It is an active ingredient in several over-the-counter formulations including Clear Eyes and Naphcon eye drops[20].

NEP has been determined simultaneously with other imidazolines with and without derivatization by spectrofluorimetric and derivative spectrophotometric methods [21] with quantitative determination. RP-HPLC has been used to determine NEP in pharmaceutical [22] formulations with other corticosteroids with by capillary electrophoresis together with their degradation products [23] and other antibiotics and corticoids [24].

When this combination of active principles is used in pharmaceutical formulations, a problem may occur to the pharmaceutical analyst in charge of quality control. If those active principles are in small concentrations, extreme precautions should be taken in the selection of the more advantageous analytical method. To solve this problem through the application of a rapid method, but meeting the proper demands of quality control (accuracy, precision, sensitivity, and specially selectivity), when more than one active principle is involved, as in this case, a deep analytical development is required.

In this work a new convenient sensor for drug, based on aggregation of citrate- capped AuNPs is presented. The presence of BET and NEP in optimum condition induces the aggregation of AuNPs, leading to a color change from red to blue. Resulting in forming bigger size of nanoparticles, declaring an obvious color change from red to blue with increasing the concentration of BET and NEP. Different in kinetic profiles of aggregation (monitored absorbance increase versus time at 640 nm) were applied for simultaneous analysis of NEP/ BET using PLS regression as an efficient multivariate calibration. Experimental conditions were optimized to obtain the highest yield for nanoparticle formation. PLS regression as an efficient multivariate spectral calibration method was employed to make a connection between the SPR spectra of the generated AuNPs and concentration of drugs. The number of PLS latent variables was optimized by leave-one-out cross-validation utilizing prediction residual error sum of square (PRESS). The proposed model exhibited a high ability for prediction of BET and NEP concentration in samples notably, a good selective recognition of BET and NEP in kinetic data with aggregation assay was shown against other drugs. The results of this work provide a rapid method for simultaneous evaluating the quantitative analysis of BET and NEP in human plasma and eye drops at physiologically meaningful concentrations.

Scheme 1

Scheme 1: Structure of A) Betamethasoneleft, B) Nephazolineright.

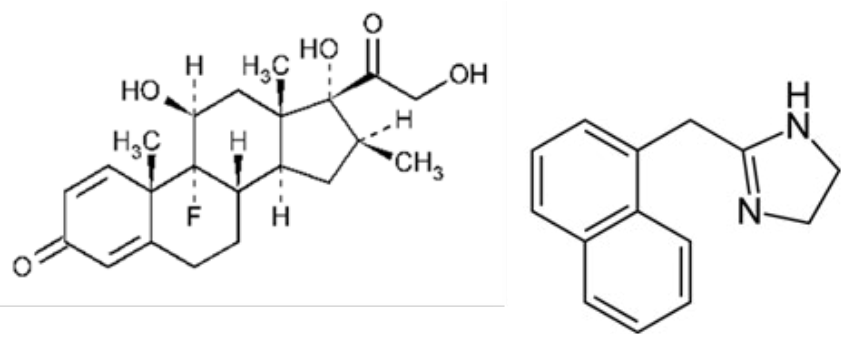

Chemicals and Materials

All materials and reagent used were of analytical grade, solvents were of spectroscopic grade and double distilled water (DDW) was used. BET and NEP pure drug were obtained from Department of Food and Drug Administration, Urmia, Iran. All chemicals used in the experiments were of analytical grade and were used without further purification. Tri sodium citrate dehydrate, HCl, NaOH were obtained from Merck (Darmstadt, 91 Germany).

Apparatus

Absorption spectra were recorded on an Agilent 8453 UV-Visible Spectrophotometer with a 1cm quartz cells. The size, morphology and structure of the synthesized AuNPs were characterized by transmission electron microscopy (TEM, Philips-CMC-300 KV). A Metrohm model 713 pH-meter was used for pH measurements. A40 kHz universal ultrasonic cleaner water bath (RoHS, Korea) was used. All calculations and programming were performed in MATLAB (Hyper-cube Inc. Version10) PLS mfiles and use essential regression.

Synthesis of gold nanoparticles

The Au seeds were synthesized according to Ferns method. Briefly, an aqueous solution 100 ml of 1 mM HAuCl4 was heated to boiling with stirring; then 10 ml 1% (w /v) aqueous sodium citrate was added suddenly. The color of the mixed solution changed from yellow to wine red in several minutes, indicating the formation of AuNPs. The boiling and stirring were continued for 15 min [25]. The seed solution was cooled to the room temperature and was stored in a dark bottle at 4°C the solution of as-prepared citrate-capped AuNPs is wine red, and has a characteristic localized surface Plasmon resonance (LSPR) absorption band of AuNPs at 520 nm (λmax) with narrow peak half-width. In solution, monodisperse AuNPs appear red and exhibit a relatively narrow surface Plasmon absorption band centered at around 520 nm in the UV-Vis spectrum (Fig. 1). In contrast, a solution containing aggregated AuNPs appears blue in color, corresponding to a characteristic red shift in the surface Plasmon resonance to higher wavelength in 640nm [26].

Fig. 1: a) TEM of AuNPs, b) TEM of aggregated AuNPs: ionic strength 1 mmol / L, time 10 min, pH of 6: AuNPs, 10 n mol / L.

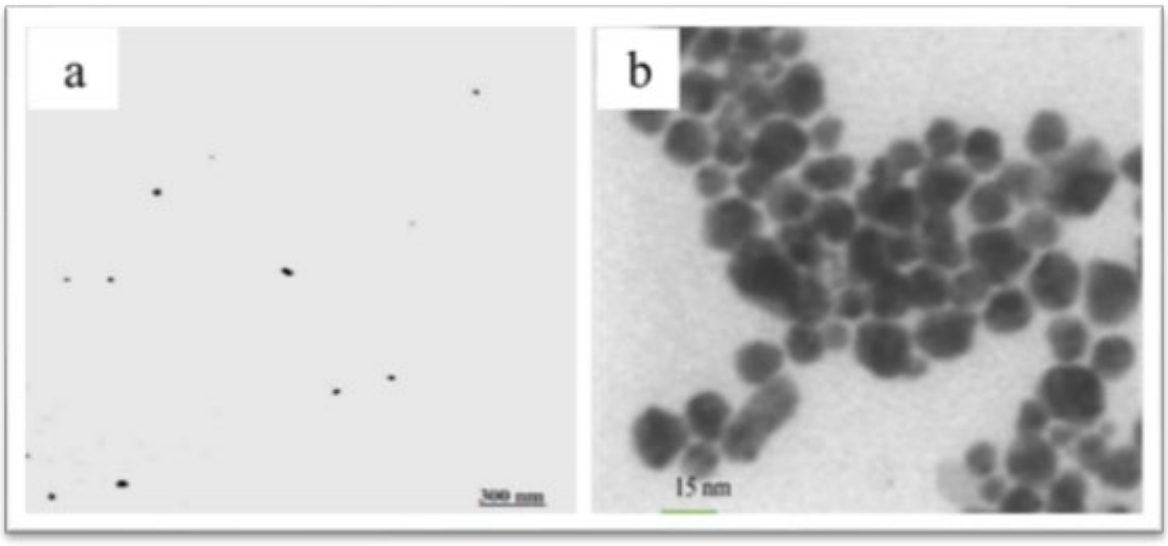

Results and discussion

Optimization of NaCl Concentration

These nanoparticles are normally charged and very sensitive to changes in the dielectric of the solution. For example, for citrate stabilized particles, the addition of NaCl shields the surface charge and leads to a concomitant decrease in the inter-particle distance and eventual particle aggregation [27].

Ion strength has a crucial role in the aggregation process that can be attributed to the ability of strong electrolytes to constrict the aroused electrical double-layer from the capping agent. Also, it is found that by increasing the ion strength above a certain limit, the aggregation of nanoparticles induces even in the absence of analytes [28]. Therefore, some controlled experiments were conducted that have revealed the concentration of 1 m mol / L of NaCl as optimized (Fig. S1) in which there is aggregation not in the absence, but only in the presence of our analytes.

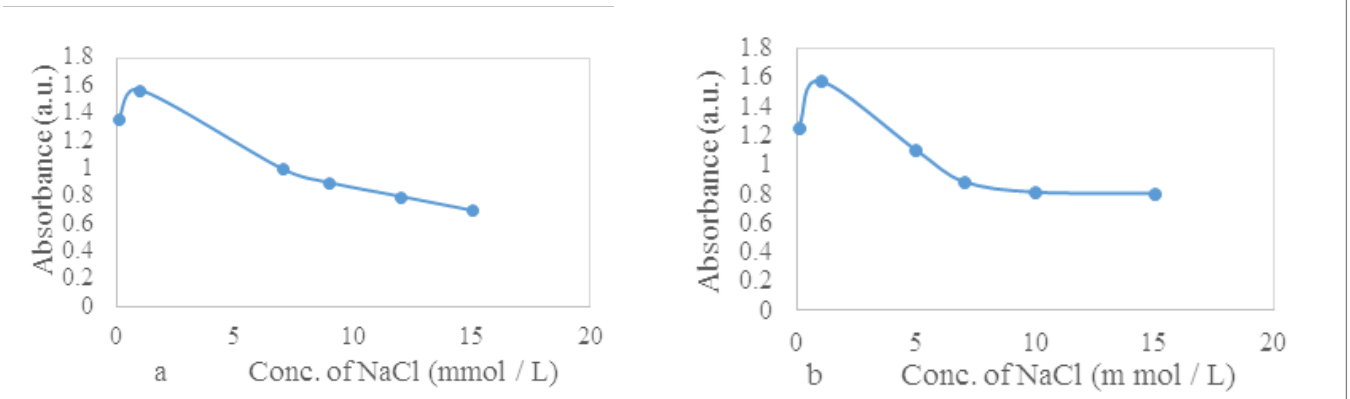

Fig. S1: Optimization of ionic strength for a) BET and b) NEP, NaCl concentration from 0.05-12 m mol / L for BET and 0.05-15 m mol / L for NEP, time 10 min, pH of 6, injection of 200 µL of BET and NEP (10-4 mol / L): AuNPs, 10 n mol / L.

Optimization of pH

Because of the presence of hydroxyl, amine and other functional groups in drugs, pH is another critical parameter that should be taken into consideration. Electrostatic interactions are the mainly responsible for aggregation of AuNPs in the presence of drugs [28]. With this in mind, to increase the possibility of electrostatic interaction, the best condition is attainable in which the drugs molecule is available in the nanoparticle surrounding. This also could be confirmed based on the stock diagram of our drugs. As shown in Fig. S2, the synthesized AuNPs are stable in the range of pH 6. Therefore, our drugs have best structure for interaction with AuNPs in of pH 6 and 7 [29, 30]. In upper alkaline pH, AuNPs attend to form hydroxide form [31] therefore the best pH for our work will be 6 (Fig. S2).

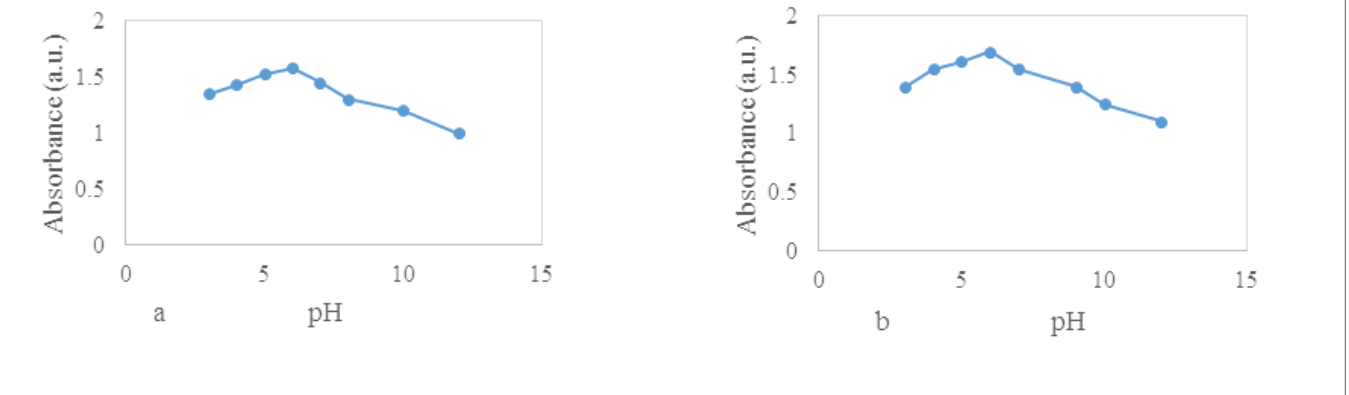

Fig. S2: Optimization of pH for a) BET and b) NEP, pH from 3-12, time 10 min, pH of 6, injection of 200 µL of BET and NEP (10-4 mol / L): AuNPs, 10 n mol / L.

Optimization of incubation time

Different incubation times were examined to find the optimized it. The results indicated that AuNPs aggregated right after mixing with BET and NEP (aggregation agent) in optimum conditions. On the other hand, the aggregation of AuNPs was suppressed and spectral change is detectable in the 10 min as an optimum incubation time. So we used this time as the end time for kinetically data that collected for simultaneously determination (Fig. S3).

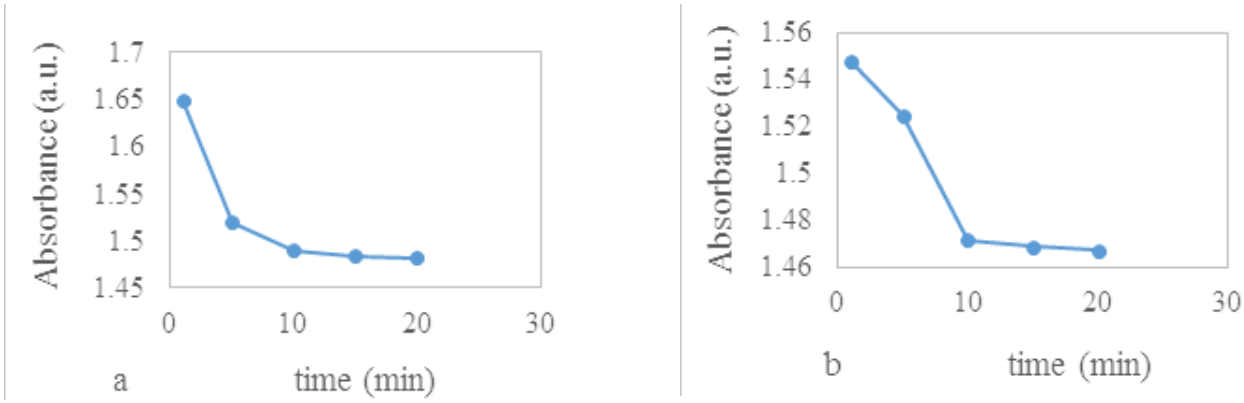

Fig. S3: Optimization of incubation time for a) BET and b) NEP, time from 1-20 min, time 10 min, pH of 6, injection of 200 µL of BET and NEP (10-4 mol / L): AuNPs, 10 n mol / L.

Partial Least Squares (PLS) Method

Partial least square regression (PLSR) calibration for both drugs was structured by using the non-linear iterative partial least squares (NIPALS) algorithm. To choose the calibration samples, the components to be determined have been selected in order to span all dimension. A training set of 26 standard samples was taken from different mixture of BET and NEP. The correlation between the different calibration samples has to be avoided because collinear component in training set data will tend to cause under-fitting in PLS models [32]. The optimum number of PLS latent variables was obtained by leave one-out cross-validation utilizing prediction residual error sum of squares (PRESS) as a statistical criterion.

Method validation

For these purpose, under the optimum experimental conditions, a typical calibration curve was obtained for the determination of BET and NEP by plotting absorbance (A) signal vs. drugs concentrations. The calibration curve was linear in the range of 0.05-13 µg / mL and 13-133.3 µg / mL with y = - 0.031 x + 1.5332, R2 = 0.9907; y = - 0.0037 x + 1.8116, R2 = 0.9906 (Fig. 2) the detection limit is 0.15 µg / mL (n=5) for BET and 0.03 µg / mL for NEP (Table 1). Table 2 shows a comparison between the results obtained by the present method with those obtained by some other methods reported for the determination of these drugs. As compared in Table 2, the present method has a good detection limit and the linear range compared with Rapid Derivative Spectrophotometric Method ,Validated spectrophotometric and chemometric methods, micellar electro kinetic chromatography, Integrated Analytical Tools Spectrophotometric, chemo metric and chromatographic determination, LC-MS/MS, validated liquid chromatographic method, high performance liquid chromatography (HPLC) and RP-HPLC [33-41]. It should be highlighted that the major advantages of this method is using of very simple method for simultaneously determination of this drug.

Table 1: Method validation parameters for BET and NEP, respectively

Equation	y = - 0.031 x + 1.5332, y= - 0.0037 x + 1.8116
R^2	0.9907, 0.9906
LOD	0.006 and 0.14 µ g / mL
Linear range	0.05-13 µg / mL and 13-133.3 µg / mL

Table 2: Characteristic performance data obtained by spectrophotometric method and other techniques for determination of NEP and BET.

Detection method	Linear range (µg / mL)	LOD (µg / mL)	Reference
a) NEP			
Rapid Derivative Spectrophotometric	0.2-1	0.03	[33]
Validated spectrophotometric and chemo metric	0.2-2	0.01	[34]
micellar electrokinetic chromatography	0.08-10	0.004	[35]
Integrated Analytical Tools	5-35	0.06	[36]
Spectrophotometric, chemometric and chromatographic	0.5-100	0.06	[37]
b) BET			
LC-MS/MS [a]	2–32	0.53	[38]
validated LC[b]	15-150	6.1	[39]
HPLC[c]	5-200	1.5	[40]
RP-HPLC[d]	0.1-100	0.025	[41]
Simple spectrophotometric method	(BET) 13-0.05 (NEP)13- 133.3	(BET)0.006 (NEP) 0.14	This work

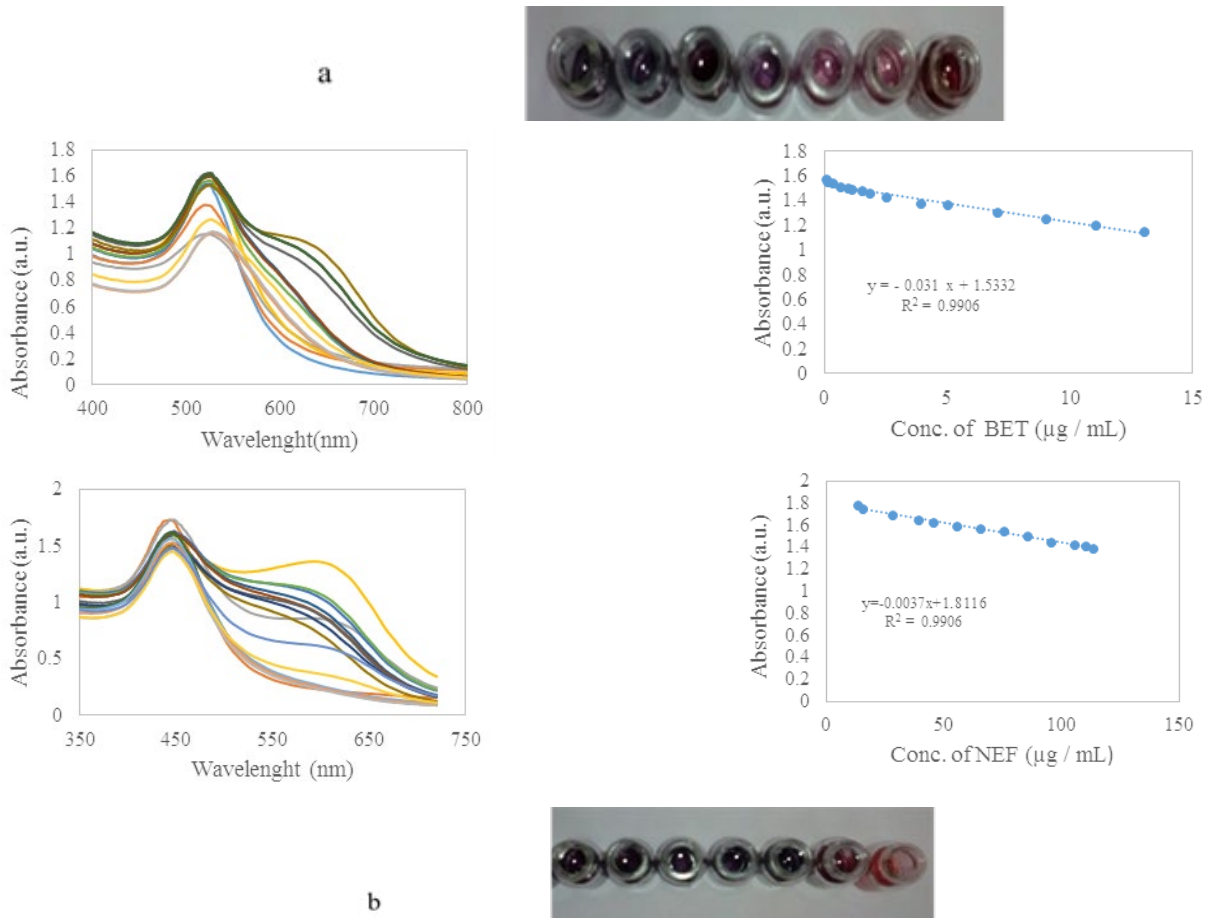

Fig. 2: Calibration curve a) for BET 0.05-13 µg / mL and b) for NEP 13-133.3 µg / mL, respectively: ionic strength 1 mmol / L, time 10 min, pH of 6: AuNPs, 10 n mol / L.

The first step in simultaneous determination of different metal ions by PLS methodology involves construction the calibration set for the double mixture chosen so that the absorbance's obtained for all standard samples were not more greater than 2. A number of 26 double mixtures of BET and NEP were selected as calibration set. Their composition was randomly designed for obtaining more information from the calibration procedure. Under these conditions, the calibration models were obtained. The obtained model was validated with a 7 samples as prediction set in different proportions of our drugs that were randomly selected. To select the number of factors in the PLS algorithm, a cross-validation method, leaving out one sample at a time, was employed [42]. For the mentioned sets of 19 calibration spectra, PLS-1 and PLS-2 was performed and, using this calibration, the amount of the sample left out during the calibration process was obtained. This process was repeated 26 times and each sample has been left only once. The amount of each sample was then predicted and compared with the known values. Preliminary investigations showed that increasing at 640 nm is directly related to the level of BET and NEP in sample (Fig. 3, 4). This irregularity can be attributed to the interfering effect of the other constituents, which can aggregate Au+3 and produce AuNPs with bigger size. Thus, we employed PLS regression as a powerful and mostly used multivariate calibration method to model the contribution of the interfering species in the total SPR signals. The PLS model was developed using the calibration set, Changes in PRESS and as a function of the number of PLS latent variables are given in Fig. 5. In addition, the first plate au in PRESS is observed at the number of latent variables of 7. Accordingly, seven principal components were chosen to calculate the PLS regression coefficients and to predict the BET and NEP content of prediction samples. The root mean square error of cross- validation (RMSECV) estimated by this number of latent variable was 2.92%. Among the detected factors, one can be related to the BET and another related to NEP. In addition, nonlinearity in the absorbance–concentration relationship and interaction between the factors can be considered as the other sources of chemical factors. The predicted values of NEP and BET level in the calibration and prediction samples and their corresponding relative errors of prediction are listed in Table 3, 4 and 5. It is observed that the predicted values are very close to the actual amount and the relative prediction errors are almost lower than 5.0%. This confirms the success of the PLS regression for accurate prediction of BET and NEP amount in samples. Now, it will be beneficial to compare the results of PLS1 and PLS2 multivariate calibration resulted in a more appropriate model or not. For this comparison and the validation of the models, some statistical parameters including root mean square error of prediction (RMSEP), root mean square error of cross validation (RMSECV) and root mean square error of calibration (RMSEC) were calculated [43–47].

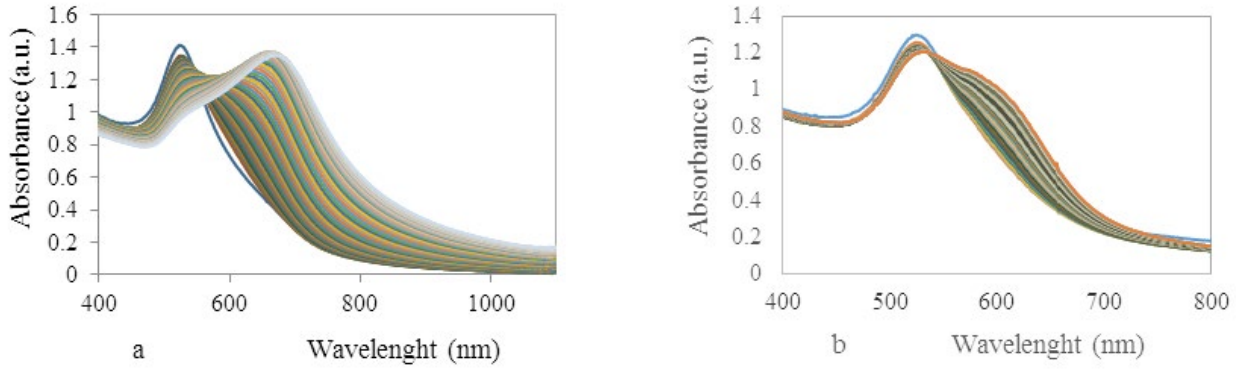

Fig. 3: Change in absorbance of AuNPs at 520 and 640 nm with time, for injection of BET and NEP (700 µL solution 10-4 mol / L) in each optimum condition of these drugs: ionic strength 1 mmol / L, time 10 min, pH of 6: AuNPs, 10 n mol / L.

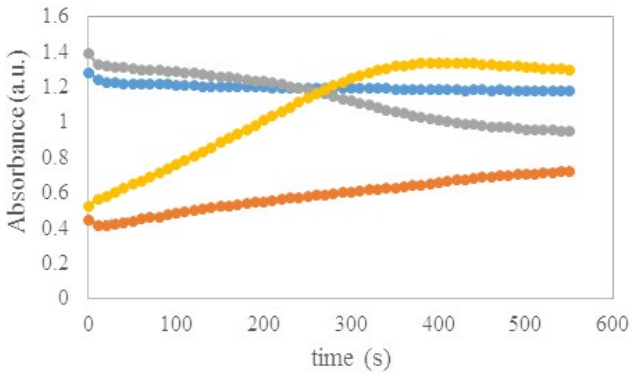

Fig. 4: Change in absorbance of AuNPs at 520 and 640 nm with time, for injection of BET and NEP (700 µL solution 10-4 mol / L) in each optimum condition of these drugs: ionic strength 1 mmol / L, time 10 min, pH of 6: AuNPs, 10 n mol / L.

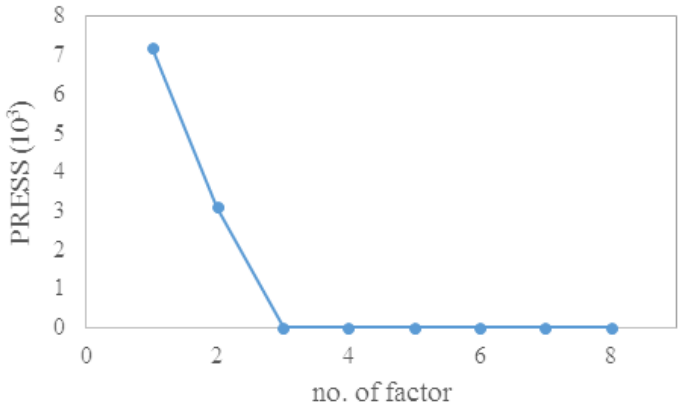

Fig. 5: Plot of PRESS against the number of factors for BET and NEP.

Table 3: The level of reference value of NEP and BET in the prediction set by PLS modeling of UV-Vis spectra at 640 nm.

prediction set						
No.	Reference value of NEP	Reference value of BET	Predicted value			
			PLS_1		PLS_2	
1	650	550	651.8844	557.722	651.8869	557.7127
2	510	400	508.3715	401.9272	508.358	401.9882
3	330	200	327.9525	184.5417	327.9727	184.4577
4	300	650	297.4573	648.9611	297.4618	648.9475
5	560	750	562.532	745.1088	562.5399	745.0587
6	230	150	228.1729	150.5885	228.1921	150.5015
7	450	450	450.0443	454.4034	450.0187	454.5119
R.S.E. (%)			0.42	1.42	0.43	1.43
$R.S.E.(\%) = \left[\frac{\sum_{j=1}^{N}(c\hat{}j-cj)2}{\sum_{j=1}^{N}(cj)2}\right]1/2\times100$						
$R.S.E.t(\%) = \left[\frac{\sum_{j=1}^{M}\square\sum_{j=1}^{N}(c\hat{}ij-cij)2}{\sum_{j=1}^{M}\square\sum_{j=1}^{N}(cij)2}\right]1/2\times100$						1.08

Table 4: The level of reference value of BET and NEP in the calibration set by PLS modeling of UV-Vis spectra at 640 nm.

calibration set						
No.	Reference value of codeine	Reference value of morphine	Predicted value			
			PLS_1		PLS_2	
1	320	260	317.6658	257.8081	317.6431	257.8065
2	270	145	273.9307	149.9602	273.7931	150.0102
3	630	810	654.5072	841.9407	653.9682	842.2023
4	580	735	578.8586	739.5673	578.7973	739.5964
5	210	270	207.1127	262.7158	207.2249	262.6609
6	280	340	278.658	359.5046	278.7915	359.4397
7	240	300	234.2856	299.5641	234.398	299.5092
8	260	340	255.2695	329.6023	255.3876	329.5449
9	390	460	379.8228	448.5799	380.0658	448.4583
10	370	470	359.2038	456.8963	359.3852	456.8076
11	300	380	296.8292	377.3036	296.8404	377.2977
12	570	730	584.1526	736.5923	584.0074	736.6613
13	370	470	360.597	454.9917	360.8028	454.8908
14	230	290	221.2696	277.4416	221.3903	277.3823
15	220	290	216.2249	276.5927	216.3373	276.5379
16	410	530	406.7595	523.0292	406.9464	522.9381
17	250	320	240.0657	309.1296	240.1824	309.0728
18	210	280	209.5112	273.9288	209.6056	273.8832
19	260	330	252.6812	323.6239	252.7918	323.5699
R.S.E. (%)			2.44	2.71	2.39	2.73
$R.S.E.(\%) = \left[\frac{\sum_{J=1}^{N}(C\hat{}j - Cj)2}{\sum_{J=1}^{N}(Cj)2}\right] 1/2 \times 100$						
$R.S.E.t(\%) = \left[\frac{\sum_{J=1}^{M} \sum_{J=1}^{N}(C\hat{}ij - Cij)2}{\sum_{J=1}^{M} \sum_{J=1}^{N}(Cij)2}\right] 1/2 \times 100$						2.61

Table 5: Statistical parameters of the PLS1 and PLS2 calibration models developed for simultaneously determination of NEP and BET with kinetic data.

	Model of prediction	
Statistical parameters	PLS_1 (%)	PLS_2 (%)
RMSEP	3.01	3.05
RMSECV	2.91	2.92
RMSEC	4.96	4.99

Interference study

The influences of foreign coexisting substances such as naproxen, ascorbic acid, tramadol, codeine, acetaminophen, saccharides, amino acids and ions were tested. . From the results, the interference of naproxen, ascorbic acid, Na_2NO_2, tryptophan, tyrosine, glucose, sucrose, fructose and lactose were very weak (as species number 1 in Fig. 6). Among the tested substance K^+, Na^+, NO_3^-, I^-, Cl^-, Mg^{2+}, Fe^{3+} and Ca^{2+} , codeine and cysteine (Fig. 6 species number 2) can be allowed with relatively higher concentrations but Cefexime, Ceftriaxone, Antazoline, NH_2OH, Mn^{2+}, Cd^{2+}, SO_4^{2-}, Ca^{2+}, Zr^{2+}, Co^{2+}, Zn^{2+}, Ni^{2+}, Al^{3+}, Fe^{2+}, Cu^{2+} can only be allowed with relatively moderate concentrations (species number 3 in Fig. 6). The allowed concentrations of these interfering substances however, were still rather higher than that of BET and NEP which indicated that this method had a good selectivity between drugs and other species because of difference in decreasing and increasing spectra with time.

Fig. 6: Tests for interference substance on simultaneous determination of BET and NEP (mixture 200 µL of BET and NEP mixture, respectively and amount of interference species also 200 µL; in optimum condition: ionic strength, 1 mmol / L, time 10 min, pH of 6: AuNPs, 10 n mol / L, 1, 2, 3 are number of species in text. 4 is behavior of BET and NEP in mixture.

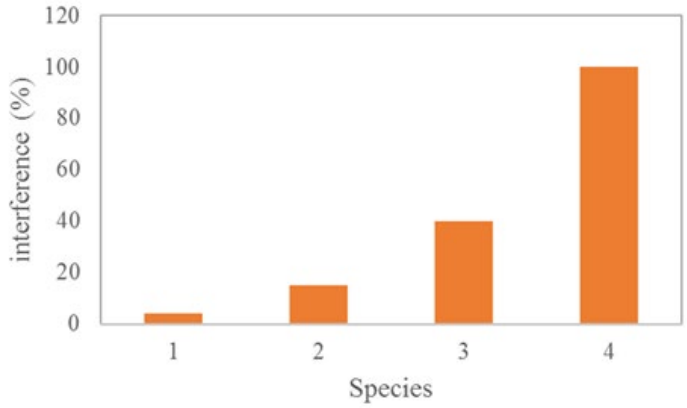

Real sample analysis

In order to test the applicability of the proposed method, it was applied to determination of BET and NEP in spicked serum and eye drop samples. The constructed PLS model was applied to estimate the concentration of BET and NEP in these spicked samples. The results that have been achieved show good recoveries (98.3-101.6). The results demonstrated the potential applicability of this method for simultaneous detection of BET and NEP in in serum, and eye drops. The results for this assay are given in Table S1.

Table S1: Analysis of diluted blood serum sample and eye drops for both BET and NEP: ionic strength 1 mmol / L, time 10 min, pH of 6: AuNPs, 10 n mol / L.

sample	add (µg / mL)		Found (µg / mL)		Recovery(%)	
	BET	NEP	BET	NEP	BET	NEP
serum	0	0	ND*	ND	-	-
	5.0	15.0	4.98	15.03	99.6	100.2
Eye drops	0	0	ND	ND	-	-
	7.0	14.0	6.88	14.23	98.3	101.6

***ND: not detected**

Conclusion

The SPR of the AuNPs, synthesized by the reduction of gold ion with citrate, were used as a novel analytical method for determination of drugs and species based on aggregation of these nanoparticles. A direct relationship was found between the levels of drugs and difference in intensity of AuNPs spectra with time in λmax at about 520 and 640 nm. However, multivariate calibration modeling of the SPR absorbance data by PLS regression resulted in more accurate results so that the relative prediction errors were almost lower than 5%. In comparison with the available analytical methods for simultaneously determination of BET and NEP, the proposed method has the following advantages: (i) it needs lower amounts of reagents; (ii) since this method is selective, the method in real samples can be determined without any initial sample preparation. (iii) The proposed method has a simple, fast, and low cost procedure, in contrast to chromatographic methods, this method does not need any expensive apparatus, and (iv) compared with spectrophotometry combined with chemo metrics, both methods similarly need the minimum sample preparation steps and one cannot prefer one over another for sample preparation complexity. A visible color change of AuNPs from wine red to blue was observed with increasing the BET and NEP concentration so the obvious color change induced can be easily detected by naked eyes. The method we developed the method is very sensitive and simple without any further modification of AuNPs.

Graphical abstract

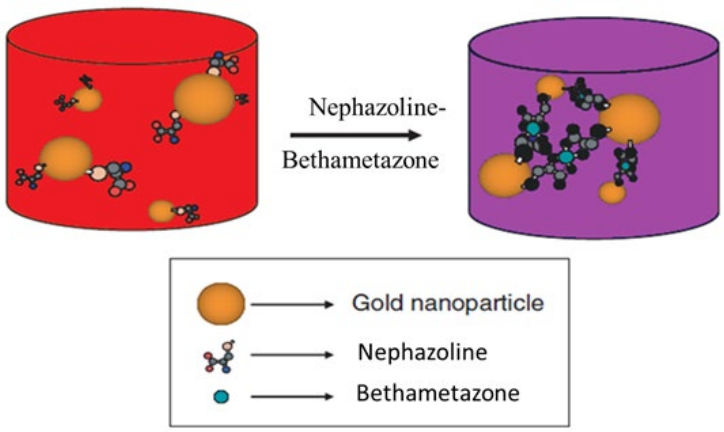

References

1. S.K. Ghosh, T. Pal, Interparticle coupling effect on the surface plasmon resonance of gold nanoparticles: from theory to applications. Chem. Rev. 107 (2007) 4797–4862.
2. I. H. Lee, H. K. Kwon, D. Kim, Colorimetric determination of copper (II) using a polyamine-functionalized gold nanoparticle probe, Angew. Chem. Int. Ed. 124 (2012) 8930–8935.
3. D. Liu, Z. Wang, X. Jiang, Gold nanoparticles for the colorimetric and fluorescent detection of ions and small organic molecules, Nano scale. 3 (2011) 1421-1425.
4. B. Liu, H. Tan, Y. Chen, Rapid and Sensitive Detection of Protein Biomarker Using a Portable Fluorescence Biosensor Based on Quantum Dots and a Lateral Flow Test Strip, Microchim. Acta. 180 (2013) 331-335.
5. D. Villa, M.C. Gonzalez, A. Escarp, Determination of polyphenolic content in beverages using laccase, gold nanoparticles and long wavelength fluorimetry, Anal. Chim. Acta. 751 (2012) 24-29.
6. Y-Q. Dang, H-W. Li, B. Wang, L. Li, Y. Wu, Selective detection of trace Cr3+ in aqueous solution by using 5,5'-dithiobis (2-nitrobenzoic acid)-modified gold nanoparticles, ACS. Appl. Mater. Interfaces. 1 (2009) 1533-1535.
[7] Y. Jiang, H. Zhao, Y. Lin, N. Zhu, Y. Ma, L. Mao, Robust Generation of Lead Compounds for Protein-Protein Interactions by Computational and MCR Chemistry: p53-Hdm2 Antagonists, Angew. Chem. Int. Ed. 49 (2010) 4800-4820.
8. Y. Jiang, H. Zhao, N. Zhu, Y. Lin, P. Yu, L. Mao, A simple assay for direct colorimetric visualization of trinitrotoluene at Pico molar levels using gold nanoparticles, Angew. Chem. Int. Ed. 47 (2008) 8601-8605.
9. Y. Zheng, Y. Wang, X. Yang, Surface imprinted macro porous film for high performance protein recognition in combination with quartz crystal microbalance, Sensors. Actuators. B. 156 (2011) 95-96.
10. K. Ai, Y. Liu, L. Lu, Monolayer-Protected Cluster Molecules, J. Am. Chem. Soc. 131(2009) 9496-9499.
11. K. R. Beebe and B. R. Kowalski, Quantitative palaeoenvironmental reconstructions, Anal. Chem. 59 (2001) 1007-1009.
12. L. Gao, S. Ren, Determination of Carcinoembryonic Antigen in Human Sera, Anal. Biochem. 405 (2010) 184-187.
13. E. V. Thomas, D. M. Haaland, compariation of multivariate calibration methods for quantitative spectral analysis, Anal. Chem. 62 (2000) 58-59.
14. A. Afkhami, M. Bahram, Cloud Point Extraction Simultaneous Spectrophotometric Determination of Zn(II), Co(II) and Ni(II) in Water and Urine Samples by 1-(2-Pyridylazo)2-Naphthol Using Partial Least Squares Regression, Microchim. Acta. 155 (2006) 403-408.
15. R. Zannolli, S. Buoni, G. Betti, S. Salvucci, Movement Disorder Society-sponsored revision of the Unified Parkinson's Disease Rating Scale (MDS-UPDRS): Scale presentation and clinimetric testing results, off. J. of the Mov. Disorder Soc. 27 (2010) 1312–1316.
16. D. Berdeu, L. Sauze, P. Ha-Vinh, C. Blum-Boisgard, Cost-effectiveness analysis of treatments for phimosis: a comparison of surgical and m edicinal approaches and their economic effect, B.J.U. Int. 87 (2001) 239–44.
17. British National Formulary, 65th Edition, Brit. Med. Assoc. Royal Pharma. Soc. of Great Britain, London, 2013, 100-110.
18. Anonymous. The United States Pharmacopoeia29 ,NF 24. Asian Edition. United States Pharm. Conv., Inc., Rockville, USA, 2006, 268-271.
19. Anonymous. The British Pharmacopoeia. The Department of Health, London, 2005, 200-210.
20. S. M. Green, Ophthalmology: Naphazoline, Tarascon Pocket Pharmacop., Jones and Bartlett, 2008, 6572-6574.[21. S.M. Sabry, M.H. Abdel-Hay, M.H. Barary, T.S. Belal, Sensitive spectrofluorimetric and spectrophotometric methods for the determination of thonzylamine hydrochloride in pharmaceutical preparations based on coupling with dimethylbarbituric acid in presence of dicyclohexylcarbodiimide, J .Pharm. Biomed. Anal. 22 (2000) 257–266.
22. R. Bocic, C. Vallejos, A. Alvarez Lueje, F.J. Lopez, Determination of prednisolone and the most important associated compounds in ocular and cutaneous pharmaceutical preparations by micellar electrokinetic capillary chromatography, J. AOAC Int. 75 (2003) 902–911.
23. J.E. Kountourellis, A. Raptouli, J.E. Kountourellis, A. Raptouli, Simultaneous determination of 2-imidazolines and other pharmaceutical substances in commercial preparations by high-performance liquid-chromatography, Anal. Lett. 21 (2001) 1361-1370.
24. A. Yesilada, B. Tozkoparan, N. Gokhan, L. Oner, M. Ertan, Development and validation of a capillary electrophoretic method for the determination of degradation product in naphazoline HCl bulk drug substance, J. Liq. Chromatogr. Relat. Technol. 21, (2000) 2575–2582.
25. W. Huang, W. Qian, P. Jain, M. El-Sayed, practical Asymmetric Henry reaction catalyzed by a chiral diamine-Cu (OAc)2 complex, Nano. Lett. 7 (2007) 3227-3324.
26. O. P. Khatri, K. Murase, H. Sugimura, photonic bandgap of inverse opals prepared from core-shell spheres, Langmuir. 24 (2008) 3787-3790.
27. J.J. Storhoff, A.A.Lazarides, R.C. Mucic, C.A.Mirkin, R.L. Letsinger, G.C. Schatz, what controls the optical properties of DNA-linked gold nanoparticle assemblies?, J. Am. Chem. Soc. 122 (2000) 4640-4650.
28. J. Conde, J. T. Dias, V. Grazu, M. Moros, P.V. Baptista, Effect of heat treatment of optical fiber incorporated with Au nano-particles on surface Plasmon resonance, J.M. de la Fuente, Front. Chem. 2 (2014) 48-50.
29.http://www.drugs.com/pro/betamethasone-sodium-phosphate-and-betamethasone-acetate.html, 2015.
30.http://dailymed.nlm.nih.gov/dailymed/fda/fdaDrugXsl.cfm?setid=6665d0e3-e35b-45e4-b0fe 24c25e26f5ad&type=display, 2015.
31. Li. Chunfang, Li. Dongxiang, W. Gangqiang, X. Jie, H. Wanguo , growth of ZnO nanowires using Au/Pd nanoparticles as catalyst, Nanoscale Res. Lett. 2011, 6, 440-450.
32. T. Madrakian, A. Afkhami, M. Borazjani, M. Bahram, Spectrochimica Acta. Part A 61 (2005) 2988.
33. E. Souri, E. Souri, M. Amanlou, M. Amanlou, H. F. Tehran University of Medical Sciences, bioactive properties of phenolics present in Oroxylum indicum-A review, Iran. Chemical and pharmacy. Bullet. 3 (2013) 12-15.
34. A. NW, M.A. Hegazy, M. Abdelkawy, R.M. Abdelfatah, Simultaneous determination of naphazoline hydrochloride, chlorpheniramine maleate and methylene blue in their ternary mixture, Pak. J. Pharm. Sci., 26 (2013) 641-648.
35. J. Maria, L. Gallego, J. Perez Arroyo, porous polymer monoliths for extraction: Diverse applications and platforms, J. Sep. Sci. 26 (2013) 650-655.
36. Y.Z. Eman Frag, G. Gehad Mohamed, F.A. Nour El-Dien, M. El-B. Mohamed, Development of a dispersive liquid–liquid microextraction method for spectrophotometric determination of barbituric acid in pharmaceutical formulation and biological samples, Pharma. Anal. Acta. 22 (2011) 200-300.
37. N. Sayed, M. Hegazy, M. Abdelkawy, R. Abdelfatah, recent developments and applications of derivative spectrophotometry in pharmaceutical analysis, Bull. Fac. Pharm., 51 (2013) 57–68.

38. I. I. Salem, I. I. Salem, M. Alkhatib, M. Alkhati, N. Najib, LC–MS/MS determination of betamethasone and its phosphate and acetate esters in human plasma after sample stabilization, Inter. Pharm. Res. Center (IPRC), Jord. J. pharm. Biomed. Anal. 56 (2011) 983-991.
39. F. Belal, M.K. Sharaf, E.Din, N. Enany, S. Saad, A validated liquid chromatographic method for the simultaneous determination of betamethasone valerate and clioquinol in creams using time programmed UV detection, Anal. Meth. 23 (2013) 930-931.
40. L. Gonzalez, G. Yuln, M.G Volonte, Determination of cyanocobalamin, betamethasone, and diclofenac sodium in pharmaceutical formulations, by high performance liquid chromatography, J. Pharm. Biomed. Anal., 20 (2000) 487–492.
41. A. Santos-Montes, A. I. Gasco-Lopez, R. Izquierdo-Hornillos, Simultaneous determination of dexamethasone and betamethasone in pharmaceuticals by reversed-phase HPLC, Chromatograph. 39 (2002) 539-542.
42. H. Abdollahi, Simultaneous spectrophotometric determination of chromium (VI) and iron (III) with chromogenic mixed reagents by H-point standard addition method and partial least square, Anal. Chim. Acta 442 (2001) 327–336.
43. K. R. Beebe, B. R. Kowalski, Quantitative palaeoenvironmental reconstructions, Anal. Chem. 59 (2001) 1007-1009.
44. L. Gao, S. Ren, Analytical Methods for Metallothionein Detection, Anal. Biochem. 405 (2010) 184-187.
45. E. V. Thomas, D. M. Haaland, Quantitative Chemical Analysis, Anal. Chem. 62 (2000) 1091-1099.
46. S. Wold, M. Sjostrom, L. Eriksson, Imaging spectroscopy links aspen genotype with below-ground processes at landscape scales, Chemo. Intel. Lab. Syst 58 (2001) 109-110.
47. S. A. Mahesar, A. A. Kandhro, L. Cerretani, A.Bendini, S. T. H. Sherazi, M. I. Bhanger, The Molecular Basis of Chemical Change Laboratory. A continuation of CHY 123. Experimental techniques and concepts in chemistry, Food Chem. 123 (2010) 1289-1290.